

Supporting Information

**Hierarchical Metal-Free Nitrogen-Doped Porous Graphene/Carbon Composites  
as an Efficient Oxygen Reduction Reaction Catalyst**

Bao Men, Yanzhi Sun,\* Mujie Li, Chaoqun Hu, Man Zhang, Linan Wang, Yang Tang,  
Yongmei Chen, Pingyu Wan,\* and Junqing Pan

National Fundamental Research Laboratory of New Hazardous Chemicals  
Assessment and Accident Analysis, Institute of Applied Electrochemistry, Beijing  
University of Chemical Technology, Beijing 100029, China.

E-mails: sunyz@mail.buct.edu.cn; pywan@mail.buct.edu.cn

Tel./Fax: +86 10 64435452

## 1. EXPERIMENTAL SECTION

The Koutecky-Levich plot can be obtained by using the Koutecky-Levich equation, which presents the relation between the inverse of measured current density ( $j^{-1}$ ) and the inverse of square-root rotation rate ( $\omega^{-1/2}$ ).<sup>1</sup>

$$\frac{1}{j} = \frac{1}{j_k} + \frac{1}{j_l} = \frac{1}{j_k} + \frac{1}{B\omega^{1/2}} \quad (1)$$

$$B = 0.62nFD_{O_2}^{2/3}v^{-1/6}C_{O_2} \quad (2)$$

Where  $j$  is the measured current density;  $j_k$  and  $j_l$  are the kinetic current density and diffusion-limited current density, respectively;  $n$  is the number of electrons transferred per oxygen molecule;  $F$  is the Faraday constant ( $F = 96485 \text{ C mol}^{-1}$ );  $D_{O_2}$  is the diffusion coefficient of  $O_2$  in  $0.1 \text{ mol L}^{-1} \text{ KOH}$  ( $D_{O_2} = 1.9 \times 10^{-5} \text{ cm}^2 \text{ s}^{-1}$ );  $v$  is the kinematic viscosity of  $0.1 \text{ mol L}^{-1} \text{ KOH}$  ( $v = 1.0 \times 10^{-2} \text{ cm}^2 \text{ s}^{-1}$ );  $C_{O_2}$  is the bulk concentration of  $O_2$  in the electrolyte ( $C_{O_2} = 1.2 \times 10^{-6} \text{ mol cm}^{-3}$ ), and  $\omega$  is the rotating speed of the electrode. The  $H_2O_2$  yields of as-prepared catalyst can be measured by RRDE measurements and calculated from the ring and disk current by using following equation (3)<sup>2</sup>:

$$H_2O_2(\%) = 200 \times \frac{I_R/N}{(I_R/N) + I_D} \quad (3)$$

Moreover, the four-electron selectivity of the catalyst was evaluated based on the  $H_2O_2$  yield. The electron transfer number can be calculated by following equation :

$$n = \frac{4I_D}{(I_R/N) + I_D} \quad (4)$$

where  $I_R$  and  $I_D$  are the ring and disk current, respectively.  $N$  is current collection efficiency of the Pt ring.  $N$  is 0.4 obtained from the reduction of  $K_3Fe[CN]_6$ .

## 2. RESULTS AND DISCUSSION

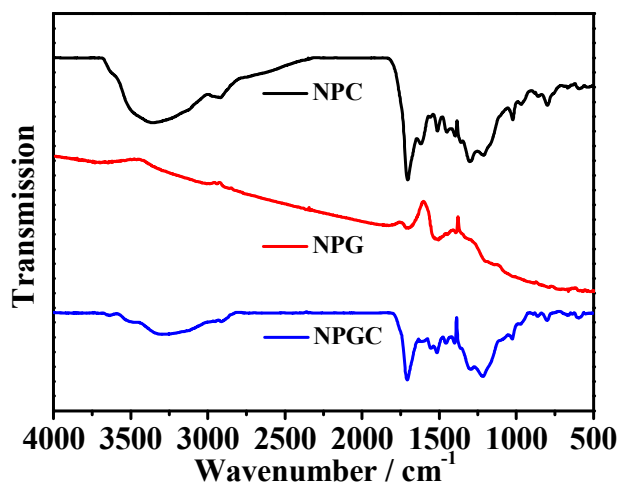


Fig. S1 FTIR spectra of NPC, NPG, and NPGC obtained after hydrothermal reaction.

Fig. S1 shows NPC has two peaks at 1708 and 1619  $cm^{-1}$ , which are attributed to C=O and C=C vibrations, respectively. These results suggest the dehydration and aromatization of glucose have occurred successfully during the hydrothermal process.<sup>3,4</sup> The NPGC has the similar IR spectra to NPC, but different from that of NPG. Combining with the SEM, the result implies reduced graphene oxide (rGO) is coated by the carbon derived from glucose. Meanwhile, the peak around 1290 $cm^{-1}$  also proves the existence of C-N bond. It demonstrates the ethylenediamine can react with hydrothermal carbon and GO so that hydrothermal carbon can tightly coat the both surfaces of rGO by the chemical bond. It is noted that the relative peak intensity of -OH ( $\sim 3360\text{ }cm^{-1}$ ) in NPGC becomes weak significantly compared with that of

NPC. The result indicates the higher degree of graphitization of glucose is achieved with addition of GO during hydrothermal carbonization reaction.<sup>4</sup>

Table S1 The mass of GO and graphene/carbon composites before and after hydrothermal reaction.

| Reactants    | Mass before           | Mass after            |
|--------------|-----------------------|-----------------------|
|              | hydrothermal reaction | hydrothermal reaction |
| GO           | 60 mg                 | 33 mg                 |
| glucose + GO | 6060 mg               | 672 mg                |

Table S2 Summary of specific surface area, pore volume and adsorption average pore size of NPC-950, NPG-950 and NPGC-950.

| Samples  | $S_{\text{BET}}/\text{m}^2 \text{ g}^{-1}$ | Pore volume/ $\text{cm}^3 \text{ g}^{-1}$ | Adsorption average pore size/nm |
|----------|--|---|---------------------------------|
| NPC-950  | 1033.85                                    | 0.61                                      | 2.34                            |
| NPG-950  | 397.37                                     | 0.41                                      | 4.12                            |
| NPGC-950 | 1510.83                                    | 0.82                                      | 2.16                            |

Table S3 Summary of the contents of C, N, and O in NPGC-750, NPGC-850, NPGC-950 and NPGC-1000.

| Samples   | Content of C<br>(atomic %) | Content of O<br>(atomic %) | Content of N (atomic %) |               |                |            |
|-----------|----------------------------|----------------------------|-------------------------|---------------|----------------|------------|
|           |                            |                            | Pyridinic<br>N          | Pyrrolic<br>N | Graphitic<br>N | Total<br>N |
| NPGC-750  | 77.74                      | 18.59                      | 1.62                    | 1.69          | 0.36           | 3.67       |
| NPGC-850  | 78.93                      | 18.01                      | 1.59                    | 1.11          | 0.35           | 3.05       |
| NPGC-950  | 81.02                      | 17.90                      | 0.26                    | 0.13          | 0.69           | 1.08       |
| NPGC-1000 | 81.71                      | 17.36                      | 0.14                    | 0.12          | 0.67           | 0.93       |

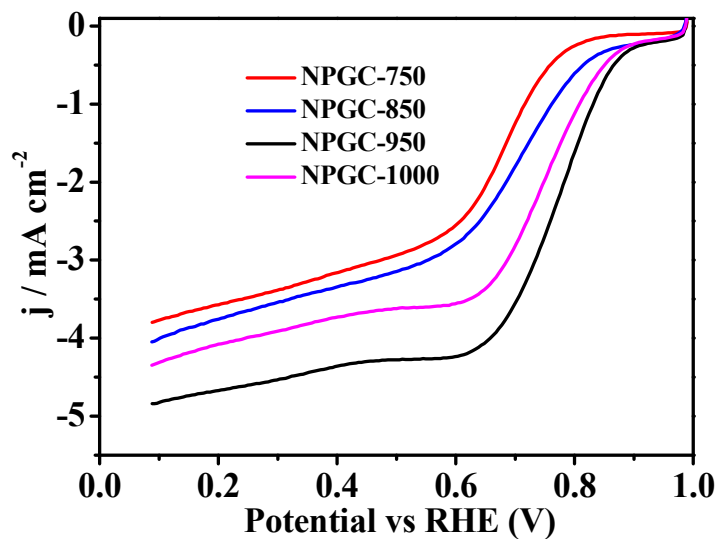


Fig. S2 LSV curves of as-prepared samples at different temperature in O<sub>2</sub>-saturated 0.1 mol L<sup>-1</sup> KOH at the rotating speed of 1600 rpm.

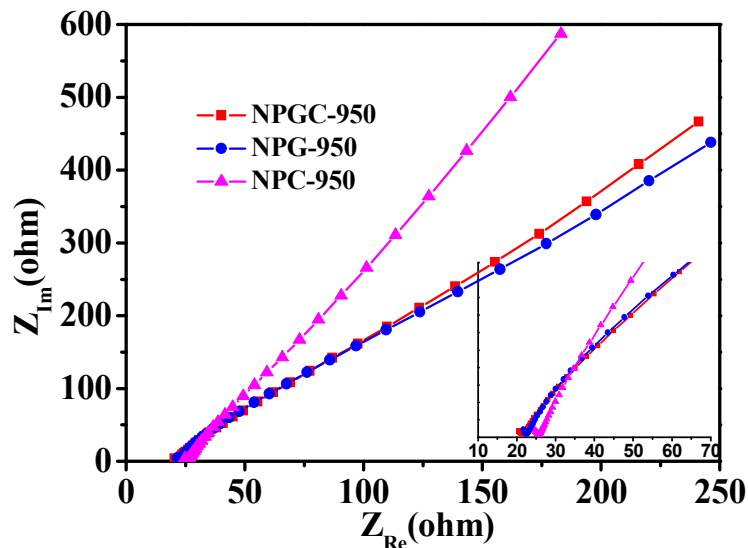


Fig. S3 Nyquist plots of NPC-950, NPG-950, and NPGC-950.

Electrochemical impedance spectroscopy (EIS) tests were analyzed by Nyquist plots of as-prepared catalysts in Fig. S2. The arc diameter in Nyquist plots at low frequency region is on behalf of the charge transfer resistance ( $R_{ct}$ ).<sup>5,6</sup> According to the Nyquist plots, it is clearly observed that the diameter of the arc of NPGC-950 is much smaller than NPC-950, very close to that of NPG-950. This result proves the introduction of reduced graphene oxide significantly enhances conductivity of NPG-950.

#### References

- (1) Zhang, P.; Sun, F.; Xiang, Z. H.; Shen, Z. G.; Yun, J.; Cao, D. P. ZIF-Derived in situ Nitrogen-Doped Porous Carbons as Efficient Metal-free Electrocatalysts for Oxygen Reduction Reaction, *Energy Environ. Sci.* **2014**, 7, 442-450.
- (2) Liang, Y. Y.; Li, Y. G.; Wang, H. L.; Zhou, J. G.; Wang, J.; Regier, T.; Dai, H.J.  $\text{Co}_3\text{O}_4$  Nanocrystals on Graphene as a Synergistic Catalyst for Oxygen Reduction

Reaction, *Nat. Mater.* **2011**, *10*, 780-786.

- (3) Sun, X. M.; Li, Y. D. Colloidal Carbon Spheres and Their Core/Shell Structures with Noble-Metal Nanoparticles, *Angew. Chem., Int. Ed.* **2004**, *23*, 597-601.
- (4) Krishnan, D.; Raidongia, K.; Shao, J. J.; Huang, J. X. Graphene Oxide Assisted Hydrothermal Carbonization of Carbon Hydrates, *ACS Nano* **2014**, *8*, 449-457.
- (5) Hou, Y.; Wen, Z.; Cui, S.; Ci, S.; Mao, S.; Chen, J. An Advanced Nitrogen-Doped Graphene/Cobalt-Embedded Porous Carbon Polyhedron Hybrid for Efficient Catalysis of Oxygen Reduction and Water Splitting, *Adv. Funct. Mater.* **2015**, *25*, 872-882.
- (6) Yu, S. P.; Liu, R. T.; Yang, W. S.; Han, K. F.; Wang, Z. M.; Zhu, H. Synthesis and Electrocatalytic Performance of MnO<sub>2</sub>-Promoted Ag@Pt/MWCNT Electrocatalysts for Oxygen Reduction Reaction, *J. Mater. Chem. A* **2014**, *2*, 5371-5378.